

# Relativistic coupled-cluster study of the parity-violation energy shift of CHFCIBr

C. Thierfelder,<sup>1</sup> G. Rauhut,<sup>2</sup> and P. Schwerdtfeger<sup>1,\*</sup><sup>1</sup>*Centre of Theoretical Chemistry and Physics, The New Zealand Institute for Advanced Study, Massey University Albany, Private Bag 102904, North Shore City, Auckland 0745, New Zealand*<sup>2</sup>*Institut für Theoretische Chemie, Universität Stuttgart, Pfaffenwaldring 55, D-70569 Stuttgart, Germany*

(Received 21 December 2009; published 22 March 2010)

Four-component relativistic coupled-cluster calculations including the nuclear spin-free electroweak field are presented for the chiral molecule CHFCIBr using a finite-field method to obtain accurate electron correlation effects for the parity-violation energy shift in CHFCIBr. The results are used to obtain optimal parameters for the Coulomb-attenuated Becke three-parameter Lee-Yang-Parr hybrid functional (CAM-B3LYP), which is useful for future applications in this field.

DOI: [10.1103/PhysRevA.81.032513](https://doi.org/10.1103/PhysRevA.81.032513)

PACS number(s): 31.15.A–, 11.30.Er, 12.15.Ji, 31.15.es

## I. INTRODUCTION

Despite the well-accepted fact that the weak neutral current between electrons and nucleons predicted by the electroweak theory creates an energy difference between two enantiomers of a chiral molecule, this kind of parity violation (PV) has never been observed experimentally [1–4]. Unfortunately, this energy difference cannot be measured directly, except for electronic transitions where the PV energy shift for the excited electronic state is zero (achiral excited state) or accidentally close to zero. One promising method is to measure PV shifts in vibrational transitions of chiral molecules [5–7]. Chardonnet and co-workers have worked to set up molecular-beam experiments using two-photon Ramsey-fringe spectroscopy with highly frequency-stable tunable CO<sub>2</sub> lasers that can reach resolutions in the mHz range [8]. Such experiments could detect PV effects for simple chiral molecules such as CHFCIBr or CHFCII (or their deuterated species) [9–12], as originally proposed by Letokhov [13]. Previous experiments by Chardonnet and co-workers were unsuccessful in detecting PV in CHFCIBr [14–16]. Another possibility is to choose chiral molecules with large PV energy shifts in the vibrational spectrum, which is currently being investigated by several research groups [17–23].

Because of the very small size of the PV energy shift, it is necessary for an experimental investigation to confirm positive outcomes from measurements by accurate theoretical predictions. Despite earlier claims that Hartree-Fock already gives reasonably accurate PV shifts for model systems such as H<sub>2</sub>O<sub>2</sub> or H<sub>2</sub>S<sub>2</sub> [24–27], it is now generally accepted that the electron correlation effect to PV is far more important than originally anticipated. Indeed, four-component Hartree-Fock (HF), Møller-Plesset second-order (MP2), and density-functional (DFT) results for *S*-CHFCIBr show large varying PV energy shifts ( $E_{\text{PV}}$ ) between the different approximations applied; that is, one obtains (in 10<sup>-18</sup> a.u.) –5.53 (HF), –2.54 (MP2), –1.54 [Becke three-parameter Lee-Yang-Parr (B3LYP)], +0.63 [Becke-Lee-Yang-Parr (BLYP)], +0.66 [Perdew-Wang (PW86)], and +2.01 [local density approximation (LDA)] [28,29]. It is evident from these results that one cannot accurately predict the PV energy shift, but the

exact value possibly lies in between the two limiting cases, the HF and the LDA result. Note that for this molecule it is not even possible to correctly predict the sign of  $E_{\text{PV}}$ . Moreover, we cannot recommend a specific density functional that gives the best PV energy shifts unless more accurate results become available. This situation is somehow similar to the problems in accurately calculating electric field gradients (EFGs) [30–35]. Note that both properties (PV and EFG) are core properties probing the wave function close to the nucleus but originating mainly from the valence orbitals [24,30].

In order to obtain accurate PV energy shifts for CHFCIBr, which is currently under experimental investigation [1,2], we performed coupled-cluster calculations using a finite-field approach for the PV operator as suggested previously by Thyssen *et al.* [25]. The coupled-cluster results were subsequently used to evaluate the quality of various density-functional approximations. Furthermore, the three parameters of the recently developed Coulomb-attenuated functional CAM-B3LYP [36] were adjusted to reproduce the PV energy shifts of the heaviest atoms in CHFCIBr as obtained by our coupled-cluster calculations. It was found in previous studies that this procedure works well for dipole moments and electric field gradients in transition-metal halides [35,37].

## II. COMPUTATIONAL METHOD

At the Dirac-Hartree-Fock and Dirac-Kohn-Sham (DKS) level, the contribution of atom *n* in a molecule to the parity violation energy shift  $E_{\text{PV}}$  can be calculated as the expectation value

$$E_{\text{PV}}^n = \langle \Psi | \hat{H}_{\text{PV}}^n | \Psi \rangle \quad (1)$$

over the (nuclear spin-independent) *P*-odd operator

$$\hat{H}_{\text{PV}}^n = \frac{G_F}{2\sqrt{2}} \sum_i Q_{w,n} \gamma_i^5 Q_n(\vec{r}_{in}), \quad (2)$$

which is derived from the timelike component of the ( $A_e$ ,  $V_N$ ) component of the  $Z^0$  exchange between electrons and nucleons;  $G_F = 2.22255 \times 10^{-14}$  a.u. is the Fermi coupling constant and  $Q_n(\vec{r})$  is the normalized nucleon density of nucleus *n*. The summation is over all electrons. The weak charge is  $Q_{w,n} = -N_n + Z_n(1 - 4 \sin^2 \theta_w)$ , where  $N_n$  is the number of neutrons and  $Z_n$  is the number of protons in nucleus *n*. For

\*p.schwerdtfeger@massey.ac.nz

the number of nucleons  $A_n = N_n + Z_n$ , values of 1, 12, 19, 35, and 79 have been used for H, C, F, Cl, and Br, respectively. The value of  $\sin \theta_W = 0.2319$  for the Weinberg mixing angle was chosen. Gaussian nuclear charge distributions for  $\varrho_n$  were chosen for the particle densities with nuclear radii taken from Ref. [38]. The Dirac-Coulomb (DC) Hamiltonian was used in all calculations [39]. All calculations were performed at the previously published coupled-cluster singles-doubles treating the triple contributions perturbatively [CCSD(T)] [40,41] optimized geometry for CHFCIBr [28] using uncontracted correlation consistent double-zeta (cc-pVDZ) and triple-zeta (cc-pVTZ) basis sets [42–44] for hydrogen, carbon, fluorine, and chlorine. Note that these basis sets already contain sufficiently hard  $s$  and  $p$  functions to correctly describe the wave function close to the nucleus. For bromine, Dyal’s double-zeta and triple-zeta basis sets augmented by hard  $p$  and  $f$  functions were utilized within the program package DIRAC [45]. The basis sets are abbreviated as DZ and TZ in the following.

Because analytical derivatives are currently not available for four-component coupled-cluster calculations, we calculate the PV expectation value for  $S$ -CHFCIBr using the finite-field method as suggested by Thyssen *et al.* [25]. The PV energy shift can be written as

$$E_{\text{PV}} = \frac{G_F}{2\sqrt{2}} \sum_n Q_{w,n} M_{\text{PV}}^n, \quad (3)$$

where  $M_{\text{PV}}^n$  is given by

$$\begin{aligned} M_{\text{PV}}^n &= \sum_i \langle \Psi | \gamma_i^5 \varrho_n(\vec{r}_{in}) | \Psi \rangle \\ &= \langle \Psi | \hat{M}_{\text{PV}}^n | \Psi \rangle. \end{aligned} \quad (4)$$

The basic idea is to deploy the PV operator as a perturbation for the HF level for the DC operator with perturbation strength  $\lambda$ ,

$$\hat{H}(\lambda) = \hat{H}_{\text{DCHF}} + \lambda \hat{M}_{\text{PV}}^n, \quad (5)$$

where  $M_{\text{PV}}^n$  is found numerically as the first derivative of the total energy of the molecule with respect to  $\lambda$ . The perturbation strength  $\lambda$  was varied over a large range ( $10^{-1} - 10^{-6}$  a.u.) and compared to analytical results at the DCHF and DCMP2 level of theory. Figure 1 shows that for  $\lambda > 10^{-2}$  a.u. the weak perturbation regime is left and  $M_{\text{PV}}^n$  drifts to larger values. For  $\lambda < 10^{-4}$  a.u., an oscillational behavior is observed due to numerical instabilities for such tiny perturbation strengths. In between, the  $M_{\text{PV}}$  values remain almost constant over a  $\lambda$  range of two orders of magnitude. For the DCHF and DCMP2 calculations, the values differ by less than 0.5% from the expectation value (Table I). This clearly indicates that the finite-field method is numerically stable and thus reliable. For the finite-field coupled-cluster calculations it was necessary to restrict the active occupied space to the valence shell (1s for H, 2s2p for C and F, 3s3p for Cl, and 4s4p for Br), and the virtual space to energies up to 100 a.u.; otherwise the calculations become computationally prohibitive. Using the smaller cc-pVDZ basis set showed that, by correlating the full virtual space, the  $M_{\text{PV}}$  CCSD value changed by less than 1%.

The wave-function-based results are compared with DKS calculations using the LDA and the functionals BLYP, B3LYP

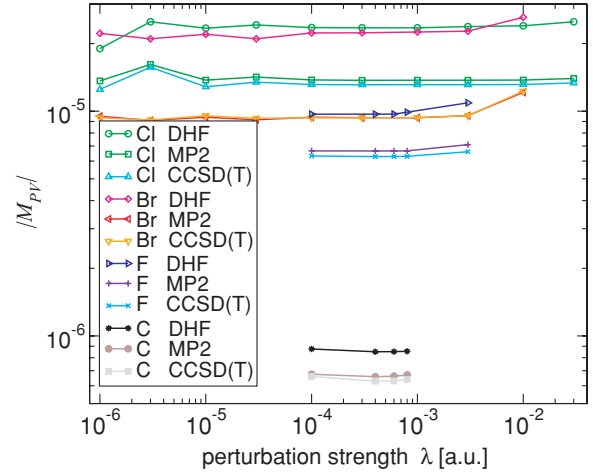


FIG. 1. (Color online) Dependence of the atomic PV contribution (in a.u.) on the perturbation strength  $\lambda$  as obtained from Dirac-Coulomb calculations.

[46,47], Perdew-Burke-Ernzerhof (PBE) [48,49], and CAM-B3LYP [36]. The CAM-B3LYP approximation [36,50] starts from a generalization of the Ewald decomposition for the electron-electron Coulomb operator into a short-range density functional and a long-range wave-function-based part [51],

$$V_{\text{ee}} = \sum_{i<j} \frac{1 - [\alpha + \beta \text{erf}(\mu r_{ij})]}{r_{ij}} + \sum_{i<j} \frac{\alpha + \beta \text{erf}(\mu r_{ij})}{r_{ij}}, \quad (6)$$

by introducing two new parameters  $\alpha$  and  $\beta$  with the constraints  $0 \leq \alpha + \beta \leq 1$ ,  $0 \leq \alpha \leq 1$ , and  $0 \leq \beta \leq 1$ . The first term accounts for the short-range interaction described by DFT, while the second term describes the long-range part through the HF exchange. The parameter  $\alpha$  determines the weight of the HF exchange for all distances, and additional long-range HF exchange is mixed in by parameter  $\beta$ . For the short-range DFT part, the B3LYP functional is used [46,47]. The original parameters ( $\alpha = 0.19$ ,  $\beta = 0.46$ , and  $\mu = 0.33$ ) for the CAM-B3LYP functional were determined to accurately produce atomization energies and charge-transfer excitations [36].

TABLE I. Comparison of  $M_{\text{PV}}^n$  Dirac-Coulomb HF and MP2 values obtained from analytical and numerical (finite-field) calculations using uncontracted cc-pVDZ basis sets for  $S$ -CHFCIBr (in  $10^{-5}$  a.u.).

Atom	Method	Analytical	Numerical
Br	HF	2.2305	2.2309
	MP2	0.9591	0.9587
Cl	HF	-2.3561	-2.3554
	MP2	-1.4131	-1.4180
F	HF	0.9701	0.9593
	MP2	0.6740	0.6702
C	HF	0.0850	0.0861
	MP2	0.0682	0.0677
H	HF	-0.0002	-0.0002
	MP2	-0.0014	-0.0013

TABLE II.  $M_{PV}^n$  values (in a.u.) for *S*-CHFCIBr obtained from Dirac-Coulomb calculations at different levels of theory using uncontracted DZ basis sets. Numbers in brackets denote powers of 10.

	Br	Cl	F	C	H
HF	2.230[−5]	−2.356[−5]	9.701[−6]	8.506[−7]	−1.875[−9]
LDA	−7.672[−6]	−5.729[−6]	1.018[−5]	1.055[−6]	−2.550[−8]
BLYP	−1.653[−6]	−9.873[−6]	1.016[−5]	8.741[−7]	−2.255[−8]
B3LYP	6.758[−6]	−1.541[−5]	1.056[−5]	9.337[−7]	−1.773[−8]
PBE	−2.567[−6]	−8.419[−6]	1.007[−5]	8.530[−7]	−2.324[−8]
CAM-B3LYP	1.208[−5]	−1.712[−5]	8.318[−6]	6.532[−7]	−1.911[−8]
CAM-B3LYP*	1.393[−5]	−1.772[−5]	7.741[−6]	6.422[−7]	−1.637[−8]
MP2	9.594[−6]	−1.413[−5]	6.740[−6]	6.820[−7]	−1.522[−8]
CCSD	1.075[−5]	−1.417[−5]	6.322[−6]	6.197[−7]	
CCSD(T)	9.346[−6]	−1.314[−5]	6.281[−6]	6.294[−7]	

### III. RESULTS AND DISCUSSION

The results of our calculations with the DZ basis set are summarized in Table II and depicted in Fig. 2. As noted before, different density-functional approximations lead to largely varying atomic PV contributions. Some functionals like LDA and PBE even yield the opposite sign for the heaviest atom, bromine, compared to the HF calculation. HF and LDA are the two limiting values for bromine, but not necessarily for the other atoms. The CCSD(T) results are close to the MP2 results, which might suggest that the latter method is sufficient to accurately describe PV effects in chiral compounds such as CHFCIBr or CHFCII. However, it is well known that single-reference MP2 fails to correct describing properties in transition-metal-containing compounds [52,53]. As chiral transition-metal compounds are already investigated for PV, single-reference MP2 may not be the method of choice for future investigations. Figure 2 shows that, out of the many DFT approximations used, the B3LYP and CAM-B3LYP functionals perform best, but the deviations are still too large to predict accurate atomic PV contributions.

It was impossible to perform a vast number of coupled-cluster calculations using the TZ basis set to find a regime for the perturbation strength where a converged PV energy difference could be obtained, and we adopted a perturbation strength of  $\lambda = 10^{-3}$  a.u., which worked well in our DZ calculations. The atomic PV contributions using the TZ basis sets are listed in Table III. For the heaviest atoms, Br and Cl, basis set effects from comparing DZ and TZ results are between 10% and 20%, and they become even larger for the lighter elements. In this

table, we also include the CCSD(T) DZ result corrected by the difference between MP2 DZ and TZ results, which are in good agreement with the CCSD(T) TZ values. Hence, this method might work well for estimating the basis set limit in PV calculations of main group element compounds.

As already mentioned, the CAM-B3LYP functional performs reasonably well, but still with rather large deviations for Br (29%), Cl (30%), and the other lighter elements. The parameters published by Yanai *et al.* [36] were determined to accurately reproduce atomization energies and charge-transfer excitations and not PV energy shifts. It was therefore necessary to reoptimize the CAM-B3LYP parameters in Eq. (5) to best describe atomic PV contributions. As DFT results are usually less basis-set-dependent than wave-function-based correlation methods such as coupled cluster, we optimized the CAM-B3LYP parameters to the CCSD(T) results of Br and Cl in a least-squares fit using the TZ basis sets (denoted here as CAM-B3LYP\*). The newly adjusted parameters are  $\alpha = 0.20$ ,  $\beta = 0.12$ , and  $\mu = 0.90$ , for which the coupled-cluster values for the Br as well as the Cl atoms were reproduced within an error of less than 5%. The final PV energy shift of  $-2.138 \times 10^{-18}$  a.u. is within 3.6% agreement with the CCSD(T) result. Note that the  $\alpha$  value is quite close to the original one proposed by Yanai *et al.* [36]. Another interesting fact is that the newly optimized parameter set to reproduce PV effects accurately in CHFCIBr differs substantially from the parameter set obtained to reproduce electric field gradients for a series of copper and gold compounds ( $\alpha = 0.4$ ,  $\beta = 0.179$ , and  $\mu = 0.99$ ). This is rather unfortunate as one wishes at least one density functional to perform well for all core properties.

TABLE III.  $M_{PV}^n$  values and total PV energy shift ( $E_{PV}$ ) obtained from Dirac-Coulomb calculations at different levels of theory using uncontracted TZ basis sets for *S*-CHFCIBr (in a.u.). The CCSD(T)/DZ + MP2/TZ value is the CCSD(T) DZ calculation corrected by the DZ/TZ difference at the MP2 level of theory. Numbers in brackets denote powers of 10.

Method	Br	Cl	F	C	H	$E_{PV}$
HF	2.159[−5]	−2.044[−5]	7.312[−6]	6.564[−7]	−1.380[−8]	−4.907[−18]
MP2	1.055[−5]	−1.710[−5]	9.610[−6]	1.090[−6]	−8.712[−9]	−1.937[−18]
CCSD(T)	1.054[−5]	−1.570[−5]	8.860[−6]	1.010[−6]		−2.064[−18]
CCSD(T)/DZ + MP2/TZ	1.030[−5]	−1.615[−5]	9.155[−6]	1.045[−6]		−1.945[−18]
CAM-B3LYP*	1.124[−5]	−1.647[−5]	8.384[−6]	7.299[−7]	−3.095[−8]	−2.138[−18]

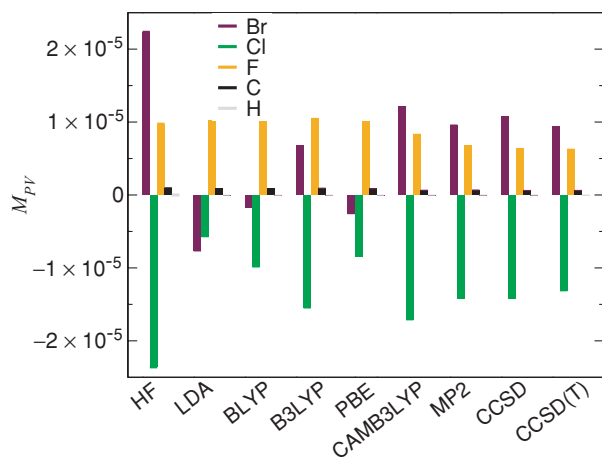


FIG. 2. (Color online)  $M_{PV}^n$  values (in a.u.) for  $S$ -CHFCIBr from Dirac-Coulomb calculations at different levels of theory using uncontracted cc-pVDZ basis sets.

To discuss the found parameter set of the CAM-B3LYP\* functional in more detail, the function  $f(r) = 1 - [\alpha + \beta \text{erf}(\mu r)]$  is plotted for the B3LYP, the CAM-B3LYP, and the CAM-B3LYP\* functional in Fig. 3. The parameter  $\alpha$  allows to incorporate the HF exchange contribution over the whole range (by a factor of  $\alpha$ ), and the parameter  $\beta$  allows to incorporate the DFT counterpart over the whole range [by a factor of  $1 - (\alpha + \beta)$ ]. The widely used hybrid B3LYP functional takes the CAM potential partitioning of Eq. (6) with  $\alpha = 0.2$  and  $\beta = 0$  [36]. The extra flexibility arising from the two extra parameters  $\alpha$  and  $\beta$  can be used to give an estimate of the importance of the HF exchange contribution for the short-range region and the DFT counterpart for the long-range region. For the CAM-B3LYP\* functional, the ratio of the DFT-HF contribution at the long-range region is shifted toward the B3LYP ratio, which means that the CAM-B3LYP\* functional is more B3LYP-like than the original CAM-B3LYP functional.

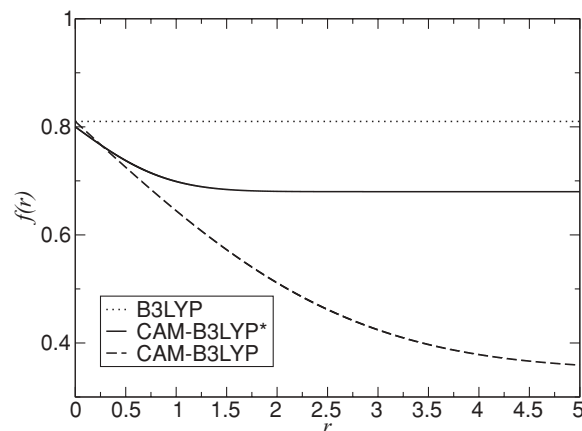


FIG. 3. Plot of  $f(r) = 1 - [\alpha + \beta \text{erf}(\mu r)]$  for the B3LYP, the CAM-B3LYP, and the CAM-B3LYP\* functionals using  $\alpha = 0.20$ ,  $\beta = 0.12$ , and  $\mu = 0.90$ .

#### IV. CONCLUSION

We presented the first coupled-cluster result for the PV energy shift in CHFCIBr using a finite-field method similar to the one described previously by Thyssen *et al.* for  $\text{H}_2\text{O}_2$  and  $\text{H}_2\text{S}_2$  [25]. None of the density-functional methods perform well, except perhaps for the B3LYP and CAM-B3LYP functionals, where deviations to the coupled-cluster results are still on the order of 30%. A readjusted CAM-B3LYP functional (CAM-B3LYP\*) using uncontracted TZ basis sets leads to atomic PV contributions in good agreement with our CCSD(T) results. This functional should be useful in future PV calculations, especially for chiral transition-metal-containing compounds.

#### ACKNOWLEDGMENT

This work was supported by the Royal Society of New Zealand through a Marsden grant.

- [1] J. Crassous, F. Monier, J.-P. Dutasta, M. Ziskind, C. Daussy, C. Grain, and C. Chardonnet, *Chem. Phys. Chem.* **4**, 541 (2003).
- [2] J. Crassous, C. Chardonnet, T. Saue, and P. Schwerdtfeger, *Org. Biomol. Chem.* **3**, 2218 (2005), and references therein.
- [3] M. Quack, J. Stohner, and M. Willeke, *Annu. Rev. Phys. Chem.* **59**, 741 (2008), and references therein.
- [4] P. Schwerdtfeger, in *Computational Spectroscopy*, edited by J. Grunenberg (Wiley, New York, 2010), and references therein.
- [5] O. N. Kompanets, A. R. Kukudzhanov, and V. S. Letokhov, *Opt. Commun.* **19**, 414 (1976).
- [6] E. Arimondo, P. Glorieux, and T. Oka, *Opt. Commun.* **23**, 369 (1977).
- [7] A. Shelkovich, C. Grain, C. Nguyen, R. J. Butcher, A. Amy-Klein, and C. Chardonnet, *Appl. Phys. B* **73**, 93 (2001).
- [8] M. Ziskind, C. Daussy, T. Marrel, and C. Chardonnet, *Eur. Phys. J. D* **20**, 219 (2002).
- [9] A. Beil, D. Luckhaus, and M. Quack, *Ber. Bunsen-Ges. Phys. Chem.* **100**, 1853 (1996).
- [10] J. Crassous and S. Hediger, *J. Phys. Chem. A* **107**, 10233 (2003).
- [11] G. Rauhut, V. Barone, and P. Schwerdtfeger, *J. Chem. Phys.* **125**, 054308 (2006).
- [12] S. Heislbetz, P. Schwerdtfeger, and G. Rauhut, *Mol. Phys.* **105**, 1385 (2007).
- [13] V. S. Letokhov, *Phys. Lett. A* **53**, 275 (1975).
- [14] C. Daussy, T. Marrel, A. Amy-Klein, C. T. Nguyen, C. J. Bordé, and C. Chardonnet, *Phys. Rev. Lett.* **83**, 1554 (1999).
- [15] C. Chardonnet, C. Daussy, T. Marrel, A. Amy-Klein, C. T. Nguyen, and C. J. Bordé, in *Parity Violation in Atomic Physics and Electron Scattering*, edited by B. Frois and M. A. Bouchiat (World Scientific, New York, 1999), p. 325.
- [16] T. Marrel, M. Ziskind, C. Daussy, and C. Chardonnet, *J. Mol. Struct.* **599**, 195 (2001).
- [17] F. Faglioni and P. Lazzeretti, *Phys. Rev. A* **67**, 032101 (2003).
- [18] P. Schwerdtfeger and R. Bast, *J. Am. Chem. Soc.* **126**, 1652 (2004).

- [19] R. Bast and P. Schwerdtfeger, *Phys. Rev. Lett.* **91**, 023001 (2003).
- [20] V. Barone and R. G. Viglione, *J. Chem. Phys.* **123**, 234304 (2005).
- [21] F. De Montigny, R. Bast, A. S. P. Gomes, G. Pilet, N. Vanthuyne, C. Roussel, L. Guy, P. Schwerdtfeger, T. Saue, and J. Crassous, *PhysChemChemPhys* (in press).
- [22] D. Figgen and P. Schwerdtfeger, *Phys. Rev. A* **78**, 012511 (2008).
- [23] D. Figgen and P. Schwerdtfeger, *J. Chem. Phys.* **130**, 054306 (2009).
- [24] J. K. Laerdahl and P. Schwerdtfeger, *Phys. Rev. A* **60**, 4439 (1999).
- [25] J. Thyssen, J. K. Laerdahl, and P. Schwerdtfeger, *Phys. Rev. Lett.* **85**, 3105 (2000).
- [26] J. K. Laerdahl, P. Schwerdtfeger, and H. M. Quiney, *Phys. Rev. Lett.* **84**, 3811 (2000).
- [27] J. N. P. van Stralen, L. Visscher, C. V. Larsen, and H. J. Aa. Jensen, *Chem. Phys.* **311**, 81 (2005).
- [28] P. Schwerdtfeger, J. K. Laerdahl, and C. Chardonnet, *Phys. Rev. A* **65**, 042508 (2002).
- [29] P. Schwerdtfeger, T. Saue, J. N. P. van Stralen, and L. Visscher, *Phys. Rev. A* **71**, 012103 (2005).
- [30] P. Schwerdtfeger, M. Pernpointner, and J. K. Laerdahl, *J. Chem. Phys.* **111**, 3357 (1999).
- [31] E. van Lenthe and E. J. Baerends, *J. Chem. Phys.* **112**, 8279 (2000).
- [32] P. Schwerdtfeger, T. Söhnel, M. Pernpointner, J. K. Laerdahl, and F. E. Wagner, *J. Chem. Phys.* **115**, 5913 (2001).
- [33] R. Bast and P. Schwerdtfeger, *J. Chem. Phys.* **119**, 5988 (2003).
- [34] P. Schwerdtfeger, M. Pernpointner, and W. Nazarewicz, in *Calculation of NMR and EPR Parameters: Theory and Applications*, edited by M. Kaupp, M. Bühl, and V. G. Malkin (Wiley-VCH, Weinheim, 2004), p. 279.
- [35] C. Thierfelder, P. Schwerdtfeger, and T. Saue, *Phys. Rev. A* **76**, 034502 (2007).
- [36] T. Yanai, D. P. Tew, and N. C. Handy, *Chem. Phys. Lett.* **393**, 51 (2004).
- [37] E. Goll, H. Stoll, C. Thierfelder, and P. Schwerdtfeger, *Phys. Rev. A* **76**, 032507 (2007).
- [38] L. Visscher and K. G. Dyall, *At. Data Nucl. Data Tables* **67**, 207 (1997).
- [39] K. Faegri and K. Dyall, *Introduction to Relativistic Quantum Chemistry* (Oxford University, Oxford, 2007).
- [40] R. J. Bartlett and M. Musia, *Rev. Mod. Phys.* **79**, 291 (2007).
- [41] L. Visscher, T. J. Lee, and K. G. Dyall, *J. Chem. Phys.* **105**, 8769 (1996).
- [42] T. H. Dunning Jr., *J. Chem. Phys.* **90**, 1007 (1989).
- [43] R. A. Kendall, T. H. Dunning Jr., and R. J. Harrison, *J. Chem. Phys.* **96**, 6796 (1992).
- [44] D. E. Woon and T. H. Dunning Jr., *J. Chem. Phys.* **98**, 1358 (1993).
- [45] DIRAC, a relativistic ab initio electronic structure program, Release 3.1, was written by T. Saue, T. Enevoldsen, T. Helgaker, J. Aa. Jensen, J. K. Laerdahl, K. Ruud, J. Thyssen, and L. Visscher; see <http://dirac.chem.sdu.dk>; T. Saue, K. Faegri Jr., T. Helgaker, and O. Gropen, *Mol. Phys.* **91**, 937 (1997).
- [46] A. D. Becke, *J. Comput. Chem.* **20**, 63 (1999).
- [47] C. Lee, W. Yang, and R. G. Parr, *Phys. Rev. B* **37**, 785 (1988).
- [48] J. P. Perdew, K. Burke, and M. Ernzerhof, *Phys. Rev. Lett.* **77**, 3865 (1996).
- [49] J. P. Perdew, K. Burke, and M. Ernzerhof, *Phys. Rev. Lett.* **78**, 1396 (1997).
- [50] M. J. G. Peach, T. Helgaker, P. Salek, T. W. Keal, O. B. Lutnæs, D. J. Tozer, and N. C. Handy, *Phys. Chem. Chem. Phys.* **8**, 558 (2006).
- [51] H. Stoll and A. Savin, in *Density Functional Methods in Physics*, edited by R. Dreizler and J. da Providencia (Plenum, New York, 1985), p. 177.
- [52] K. Raghavachari and G. W. Trucks, *J. Chem. Phys.* **91**, 1062 (1989).
- [53] M. Seth, F. Cooke, M. Pelissier, J.-L. Heully, and P. Schwerdtfeger, *J. Chem. Phys.* **109**, 3935 (1998).